Distortion Correction in LODOX StatScan X-Ray Images

Matthew Paul Beets

November 27, 2007

X-Ray images produced by the LODOX StatScan machine contain a non-linear distortion in the direction of the beam width. This thesis presents a software based method for correcting this distortion by combining the data from multiple scans of the patient at different angles.

Declaration

I, Matthew Paul Beets, know the meaning of plagiarism and declare that all the work in this document, save for that which is properly acknowledged, is my own.

Signed by candidate

Acknowledgments

I would like to acknowledge the following people for their contribution to my work:

- My parents, for letting me follow my studies.
- My supervisor, for always being ready with suggestions for progress.
- My sister, for showing me what hard work is really all about.
- My friends, for their constant support.
- Bronwyn, for being there.

Synopsis

This thesis presents a background and description of a method of distortion correction in x-ray images produced by the LODOX StatScan machine.

The distortion correction of an object's x-ray image is of particular interest in the medical field, particularly for prosthetics, implants, and orthopedic work.

It is useful to be able to take accurate measurements directly from x-ray images and that these images should be obtained with a minimum of patient discomfort and exposure to radiation.

Current x-ray images contain a non-linear distortion that must be corrected for by hand. This distortion is a result of the imaging process: X-rays from a point source spread out before being captured by a detection device such as a photographic plate or an electronic CCD sensor.

Because of this, objects closer to the center of the detector suffer less distortion than those at the edges and makes the correction process a non-trivial task traditionally requiring multiple scans to be taken and stitched together manually to minimize the distortion.

The method of distortion correction presented here is a novel approach to the problem using the LODOX StatScan machine. It uses multiple scans from the StatScan Machine to create a single completely distortion free image entirely automatically. This is a software based correction method.

It takes multiple fan beam x-ray projections and uses them to create a single virtual parallel beam x-ray image suitable for making accurate measurements with.

Contents

List of Figures

1 Introduction

In this chapter some background and introductory material is discussed. The scope of the problem is defined and the layout of this thesis is presented.

1.1 Background

X-rays were discovered by Rontgen in 1895 (Ball and Moore [1992], Wilks [1981]). They are a stream of high energy photons that pass through low density substances but are absorbed by higher density substances. Since their discovery, x-rays have become an invaluable tool in many professions. They have applications in non-destructive testing, astronomy, as well as medical imaging (Loats and Holcomb [1989]).

A medical x-ray image is formed by exposing a patient to an x-ray source and allowing the x-rays to pass through the patients body. They are attenuated according to the density of the structures they pass through. They then illuminate a photographic film or a scintillator (which converts x-rays into visible light which can then be seen by a digital camera). X-rays are used by surgeons and radiologists for preoperative planning and the non-invasive measurement of internal features.

Orthopedic surgeons find x-ray images useful for the diagnosis of bone fractures and in the design of prosthetic implants. The planning measurements are taken directly from the patients x-ray images. However, these images contain a distortion that is a result of the imaging process. This distortion occurs because of the geometric shape of the x-ray beam which passes through the patient and onto the photographic plate (Kak and Slaney [1988]).

If we compare the amount of x-rays reaching a detector for both parallel and fan beam geometries (Figure 1), we can see how the parallel beam x-ray would result in a accurate representation of the object with sharp edges. The fan beam x-ray image would have blurred edges due to some x-rays only passing through part of the object before striking the detector. This distortion is discussed further in Chapter 3.

There is a need for distortion free x-ray images so that pre-operative measurements can be made efficiently with minimum discomfort to the patient. While procedures do exist to remove the distortion from traditional x-ray images, it remains a non-trivial task.

We can see in Figure 2 one such method using a lead ruler placed alongside the area of interest. Using the known measurements from the ruler a scaling factor can be calculated and other measurements inferred. However, because traditional x-rays use either a fan or cone beam geometry, the areas towards the edge of the scan are distorted more than those closer to the centre. All such images suffer from a non-linear distortion that is difficult to correct for using current methods.

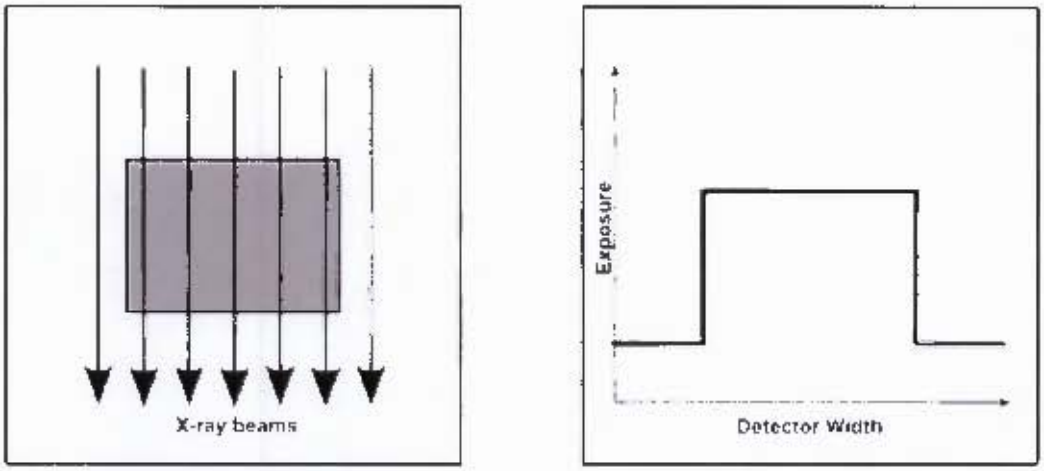

(a) X-ray exposure from parallel beams passing through an object

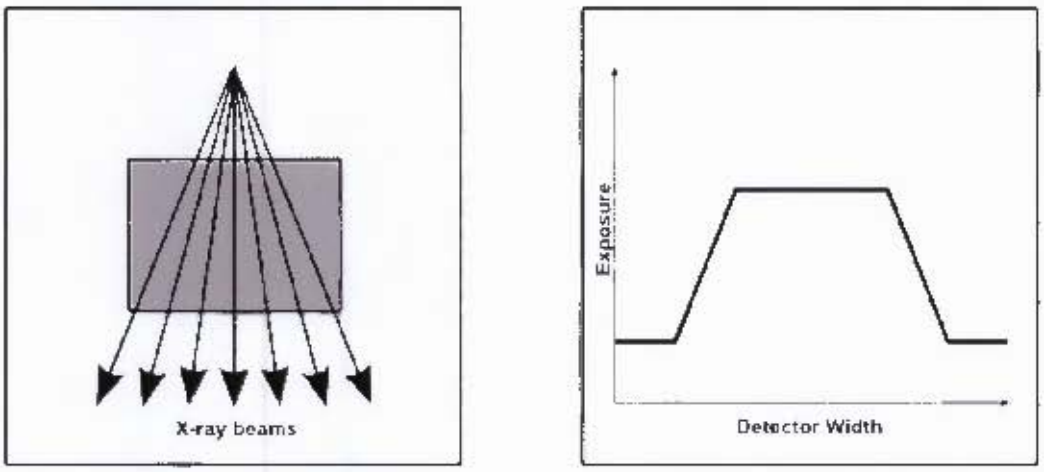

(b) Exposure from fan-beam x-rays passing through an object

Figure 1: Comparing the exposure of parallel beam and fan beam x-rays passing through equivalent objects.

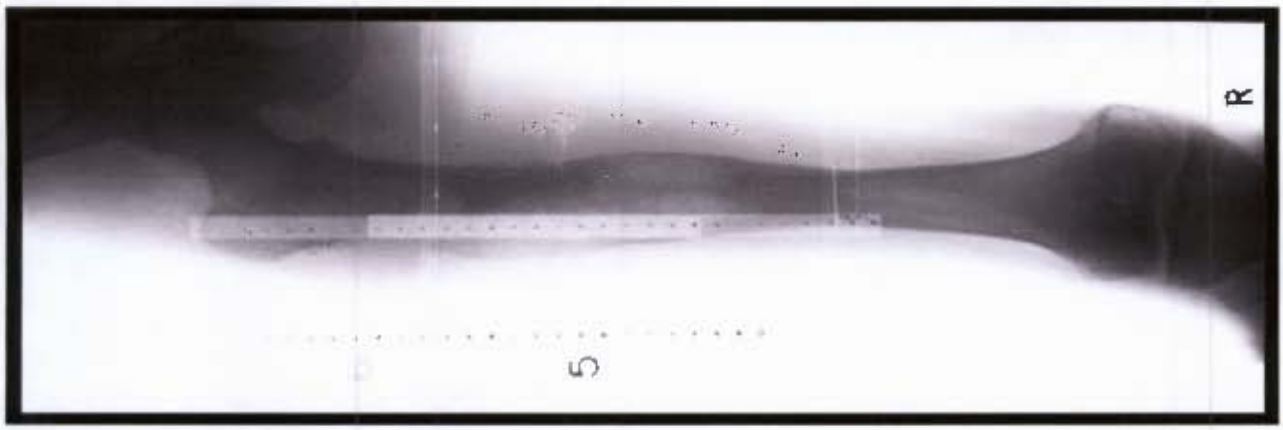

Figure 2: X-ray image with lead ruler for scale. (Colors inverted)

1.2 Method for distortion correction

This thesis presents a method of removing the distortion from traditional x-ray images by using the information from multiple scans of the patient and makes use of some elements of x-ray

tomography. An introduction to x-ray tomography is given in Chapter 2.

Figure 3: The LODOX StatScan machine.

The StatScan machine consists of a x-ray detector and source mounted on opposite sides of a c-arm. This c-arm can rotate and move linearly to scan a patient. The x-ray source produces a collimated fan beam of x-rays. This means that images produced are accurate in the scanning direction but distorted in the beam width direction.

Using the StatScan machine, multiple images of an object are acquired at different angles. The information from these fan beam x-rays is then combined to produce a single undistorted image. This computed image is what would have been seen had the x-ray been made using parallel beam x-rays.

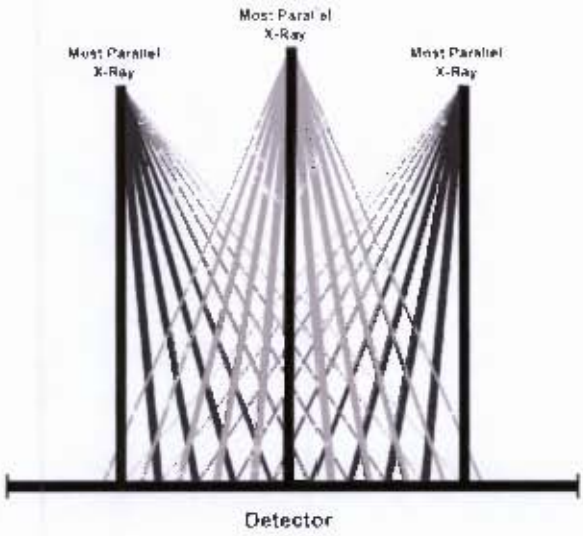

Figure 4: Multiple overlaid fan beam x-rays with rays perpendicular to the detector highlighted.

An easy way to consider the combining of information from the fan beam images to the single virtual parallel beam image is to imagine selecting the 'most parallel' information from each fan beam image. If we imagine that the detector is fixed and the source is rotating above it, then we can see (Figure 4) how in each scan some of the fan beam x-rays must strike the detector at $90°$. If we select this information from sufficient scans then we will know enough to create a single image composed entirely of parallel x-ray data.

The method presented here is discussed in more detail in Chapter 4.

The method for distortion correction presented in this thesis is specific to the StatScan machine. While the distortion present in the images does not pose a problem for the normal operation (when used for trauma analysis) of the machine, it was agreed that there was a definite advantage to be gained in increasing its utility and range of application.

Previous projects have demonstrated the possibility of using the StatScan machine for computed tomography (de Villiers [2003, 2000b,a, 1999b], Starke and de Jager [1998], Shand et al. [1998]). However due to its design the c-arm holding the detector and source cannot rotate more than 90° ,while at least 180° worth of scans are required for a good CT slice reconstruction. While the subject can be rotated and the extra angular range of scans acquired, the machine is not well suited for the task. The StatScan machine is further discussed in Chapter 3.

The distortion correction method presented here requires very few scans and is well suited for use with the StatScan machine's current mode of operation.

1.3 Problem Definition

Conventional x-ray machines tend to have one of two different beam geometries:

- A point x-ray source radiating in a cone beam towards a photographic element
- A point x-ray source radiating in a collimated fan beam towards a photographic element.

The diverging nature of the x-ray beams introduces a non-linear magnification distortion into the final x-ray image. This distortion makes taking accurate measurements directly from the x-ray images a non-trivial task. It requires manually obtaining an approximate magnification correction factor which can be used to make accurate measurements from the image.

Prosthetic implants (amongst other procedures) would benefit from a geometrically correct image from which direct measurements could be made.

Current planning procedures make use of conventional x-ray images or CT scans. The conventional x-ray images require long manual correction procedures and the CT scans are expensive and claustrophobic (although they do not have distortion or magnification errors).

An automatic distortion correction procedure is needed to create geometrically correct images from which direct measurements can be made.

1.4 Objectives

This thesis is based on work done using the LODOX StatScan Critical Imaging System. Its premise was the idea of adding value to the existing machine by creating a method to remove the distortion found in its images. This method was to be implemented in software.

A distortion correction method that used the strengths of the LODOX StatScan machine was to be created. This would be evaluated for accuracy as well as ease of use.

After initial research an approach for distortion correction was decided upon. The most promising approach involved a system that would take information from multiple fan beam scans, taken at different angles, and combine them into a single undistorted image. This was to be investigated for suitability for use in creating distortion free images. The effectiveness of the method was to to be judged by its accuracy, speed of processing as well as data collection and usefulness.

1.5 Results

A working software solution was developed according to the outlined objectives. This system took as input x-ray images produced by the StatScan machine and produced as output undistorted x-ray images suitable for diagnosis. Using the information from multiple fan beam x-rays taken at different angles of rotation (similar to a CT procedure) a single undistorted parallel beam x-ray image is produced.

Compared to the original StatScan x-rays, this processed image is geometrically accurate in the beam width as well as in the scanning direction. This was shown through taking measurements from StatScan x-ray images of calibrated metal blocks and comparing them to measurements taken from images with the geometric distortion removed.

While the image processing was initially slow, the working speed was improved dramatically during the course of this study thanks to improved techniques and more streamlined computer algorithms. The end result was a system that could, once x-ray data had been acquired, automatically calibrate the images and process them. While the processing time was influenced by both the resolution of the images and the area to be reconstructed, this was in the order of minutes rather than hours.

While the system was shown to work well on a study performed on a cadaver as well as reference objects, problems were experienced in the imaging of a live patient. This was due to movement by the patient during the x-ray process. The difficulty lies in the time that it takes to acquire the needed number of scans for the correction procedure.

A full body x-ray on the StatScan machine takes approximately 13 seconds, with any scan of a reduced portion of the body taking proportionately less time. Then the C-arm has to be rotated to the next angle and realigned horizontally over the patient before the next scan can be taken. Combined these steps can mean that acquiring a full data set for reconstruction can take up to 10 minutes.

Although the patients movements may be small and not noticeable on individual scans, they cause shearing errors in the final reconstructed image. This is especially due to any rotation of

areas under observation that may have occurred. Individual scans are vertically and horizontally aligned relative to each other but the method cannot compensate for rotational movement of the area under study. This would require a set of markers to be placed on the patient that could be used to estimate the subjects angle in every scan and correct for that movement. This was not available during this study.

This means that while this method is applicable to image areas that can be suitably immobilised it is not capable of handling areas with constant motion. It cannot be used to produce distortion corrected images of organs or the chest area.

1.6 Thesis Layout

The information in this thesis is presented with the following structure:

- In Chapter 2 a background to computed tomography is given that will form the basis for the final distortion correction implementation.
- In Chapter 3 the problem of x-ray distortion is discussed as well as the specific distortion problems associated with the LODOX StatScan machine.
- In Chapter 4 the method of correcting for the distortion present in an image taken from the StatScan machine is presented.
- In Chapter 5 a method to reduce the required number of scans needed for a distortion corrected image is introduced.
- In Chapter 6 the implementation of the distortion correction method is discussed.
- In Chapter 7 some results from the use of this distortion correction method are shown. These include calibrated studies showing the accuracy of the new method as well as its application to a live patient study.
- Finally the thesis ends with conclusions and recommendations for further work.

2 Tomography

In this chapter a brief summary of computed x-ray tomography is presented. Its application and benefits in the field of medical imaging are also discussed.

2.1 X-Ray Tomography Background

Traditional x-rays cannot show the three-dimensional shape and depth of a region. They collapse a three-dimensional structure into two dimensions, possibly obscuring features and injuries. To investigate the original structure, x-ray tomography is needed.

X-ray tomography is the reconstruction of an objects interior density distribution from its projections (Natterer [1986], Kak and Slaney [1988], Bracewell [1995]). The projections are the x-ray images of the object taken from many different angles. The problem of mathematically reconstructing a function from its projections was solved by Radon in 1917 (Helgason [1980]). This non-invasive technique allows for a cross-sectional view of the patient to be obtained. This depicts the shape and location of internal structures with great accuracy removing the ambiguity present in traditional x-ray images.

It has been shown that the StatScan machine is capable of being used to perform x-ray tomography. The x-ray source and detector pair are mounted on a mechanical c-arm which can be rotated and moved over the patient. In this way an x-ray image of the patient at any angle can be achieved. The x-ray source emits a collimated fan-beam x-ray which is detected by a bank of scintillator arrays which are optically coupled to charged coupled devices (CCD's) on the opposite side of the c-arm. The c-arm can rotate from 0 to 90 and travels along the length of the table while taking an x-ray image.

Projection data that covers a full 180-degree range viewing angle is required to produce high-resolution tomographic reconstructions. Exposure of the patient to radiation should be minimized to prevent damage to tissues. Taking a complete set of projections may also be time consuming and require a large amount of resources.

Sometimes it may be impossible to obtain projections over the full 180-degree range. Or, due to the density distribution of internal features, some projections may be greatly attenuated resulting in poor signal-to-noise ratios for that angular range. These factors encourage the use of *local*, *sparse angle*, and *limited angle* tomography (Tam and Perez-Mendez [1981], Tam et al. [1990]).

Local Tomography This is the reconstruction of a region of interest from projections for which there is only data on the region of interest and its neighborhood. Through this, significant reductions in exposure can be made with negligible distortion

Sparse Angle Tomography This is when a tomographic reconstruction is made from a small number of projections that still cover the full 180-degree range. However classical reconstruction techniques yield low resolution images with streak pattern artifacts that increase in severity as the number of projections is restricted.

Limited Angle Tomography This is where the angular range for projections is restricted. No longer are projections taken over the full 180-degree range. Classical reconstruction techniques result in distorted images that lack edge information at angles for which projection data is missing. However this is the technique best suited for use with the StatScan machine due to only being able to take 90° worth of scans before having to rotate the subject.

2.2 Radon Transform

The Radon Transform, for two and three dimensions (where a function is integrated over planes), was introduced in a paper by Johann Radon (1887-1956). We will only consider the two-dimensional case.

An x-ray beam passing through an object suffers attenuation according to the density of material that it interacts with. If the object being scanned is defined as a two dimensional function $f(x, y)$, then we can consider an x-ray passing through that object as the line integral of that function along the straight path of the x-ray. This then represents the total attenuation of the x-ray beam along that path (Kak and Slaney [1988]).

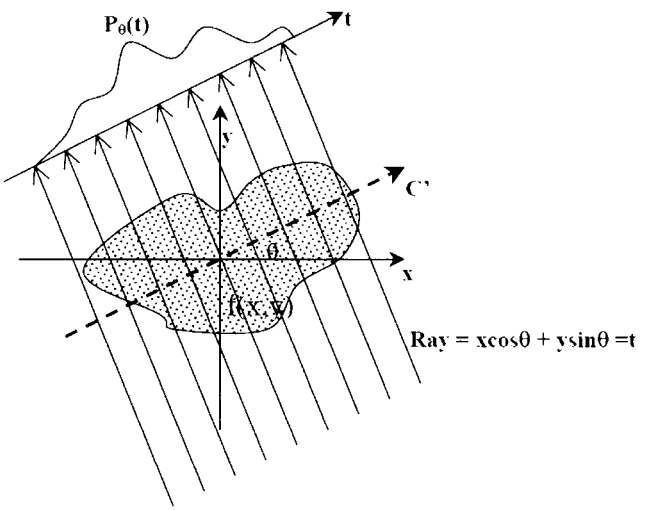

Figure 5: Parallel beam projection of an object at angle θ

As can be seen in figure 5, we can express an x-ray beam passing through an object as a line with equation,

$$x \cos\theta + y \sin\theta = t, \tag{1}$$

which can be derived from the equation for a line $y = mx + c$ with

$$m = -\frac{1}{\tan\theta} \tag{2}$$

and

$$c = \frac{t}{\sin\theta}\,. \tag{3}$$

The value of the projection at $P_\theta(t)$ is the line integral of $f(x, y)$ along this line such that

$$P_\theta(t) = \int_{(\theta,t)line} f(x, y)\, ds\,. \tag{4}$$

Using a delta function, this can be rewritten as

$$P_\theta(t) = \int_{-\infty}^{\infty}\int_{-\infty}^{\infty} f(x, y)\,\delta(x\cos\theta + y\sin\theta - t)\, dx\, dy\,. \tag{5}$$

This then is the Radon transform of the function $f(x, y)$ which is the mathematical representation of the x-ray imaging process where a projection is formed by combining a set of line integrals. These equations are for the parallel beam case.

2.3 Sinograms

When the Radon transform is performed a set of projection data is generated. This projection data can be combined with t forming one axis and θ forming the other. This collection of transform data is often called a sinogram because the Radon transform of a single point is the characteristic graph of a sine wave.

Any pixel in the original data that is offset from the origin of the image (center) will form a sine wave in the transformed data.

The equation of this sine wave is

$$t = a\sin(\theta + b)\,, \tag{6}$$

where a is the distance of the pixel from the center of rotation of the image (usually the image center) and b is the radial offset of the pixel relative to the center of rotation.

Thus the collected Radon transforms of an object at various angles θ appears as a number of blurred sine waves with different amplitudes and phases.

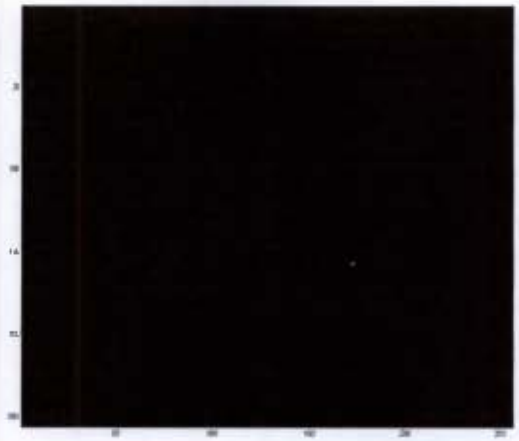

(a) Single pixel image

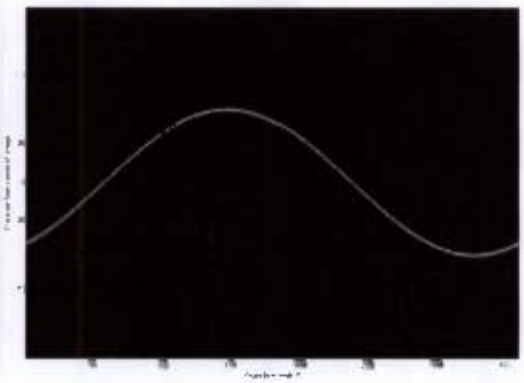

(b) Radon transfrom of a point

Figure 6: Radon transform of a single pixel image showing sine wave characteristics

2.4 The Fourier Slice Theorem

The Fourier Slice Theorem defines the relationship between the Fourier Transform of the two dimensional slice $f(x, y)$ and the projection data $P_\theta(t)$. It states:

> "The Fourier Transformation of a parallel projection of an image , taken at angle θ, gives a slice of the two-dimensional Fourier Transform $F(u, v)$, subtending an angle θ with the u-axis."

Or, the Fourier transform of $P_\theta(t)$ gives the values of $F(u, v)$ along the line shown in the frequency domain.

From this we can see that the Fourier Transforms of the projections of slice data can be used to reconstruct the complete two dimensional Fourier transform. Then, it would be possible to

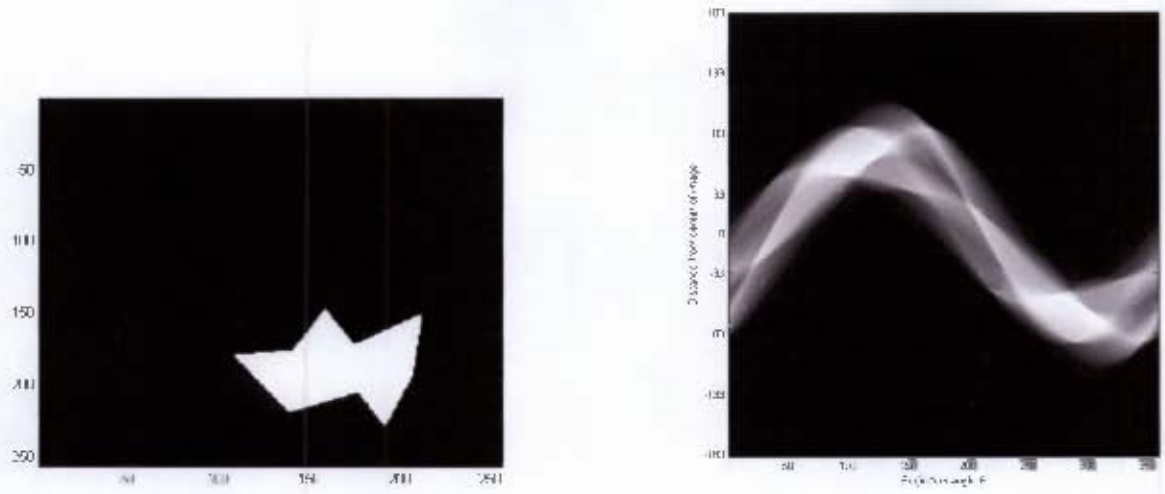

(a) Original polygon

(b) Radon Transform of Polygon

Figure 7: The Radon Transformation of an arbitrary polygon

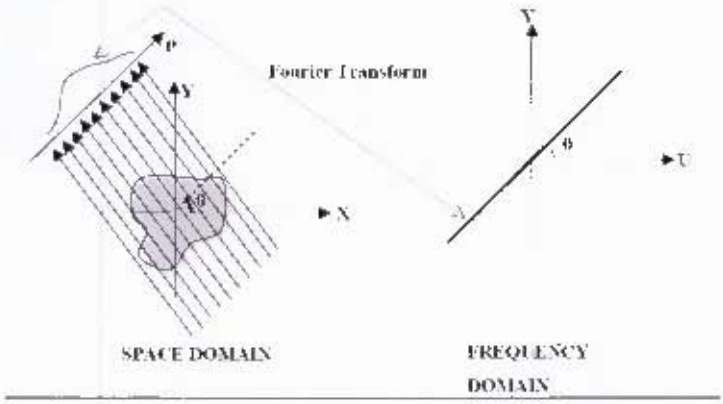

Figure 8: Illustration of the Fourier Slice Theorem.

simply perform the inverse Fourier transform to recover the original slice data (Sezan and Stark [1984]).

However an infinite number of these projections would be required for a perfect reconstruction of the Fourier transform of $f(x, y)$. In practice a limited number of projections allows for the reconstruction of the 2D Fourier Transform along radial lines of the same orientation of each projection (Figure 9).

From this we can also see why at least 180° of projection data is needed for an accurate tomographic reconstruction of the object. Without at least 180° of data there will be large gaps in the frequency domain which will introduce errors into the final reconstruction should we perform the inverse transform with them present.

We can also see that smoothing or filtering could be performed to allow for sparse angle tomography to reconstruct the original slice data. Having the full 180° of projection data a filter can be applied to weight the impact of the information in the frequency domain. The filter would

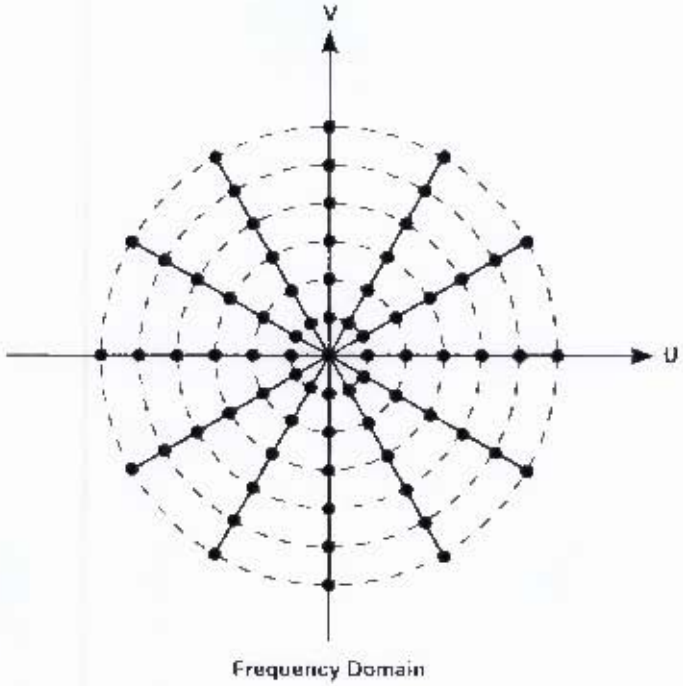

Figure 9: Projections of a limited number of angles gives an estimate of the 2D Fourier Transform of the function $f(x, y)$along radial lines.

reduce the effect of the densely clustered low frequency information and allow relatively more high frequency data to be used in the reconstruction. In practice a ramp filter can be used (Figure 11)

2.5 Filtered Back Projection

Filtered Back Projection is a simple and efficient way to recover the original slice data $f(x, y)$ from the projection data $P_\theta(t)$. It is the method most commonly used for commercial scanning equipment. For every angle θ the radon transform data is reprojected across the original image space at its corresponding angle. The original object is recreated through the constructive overlay of multiple projection data.

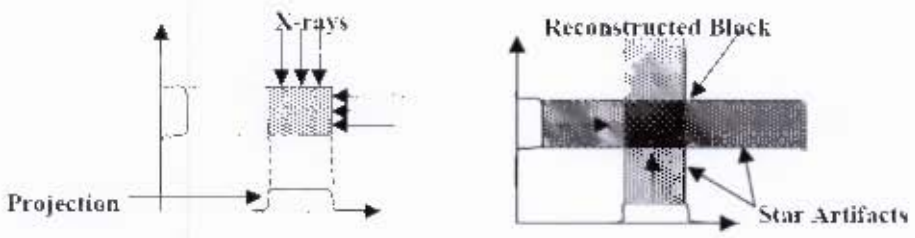

Figure 10: A block recreated from its projection data using back projection showing typical streaking artifacts.

It also produces streaking in the image known as star artifacts. The more projection overlays

that are used, the better the back projected image becomes. Filtering of the projection data can be used to remove the star artifacts from the final image.

Filtering is performed by weighting the Fourier transform of the projection data in the frequency domain. This filtering helps to eliminate the low frequency interference visible as star artifacts in the reconstructed image. One filter that can be used is an idealised ramp filter.

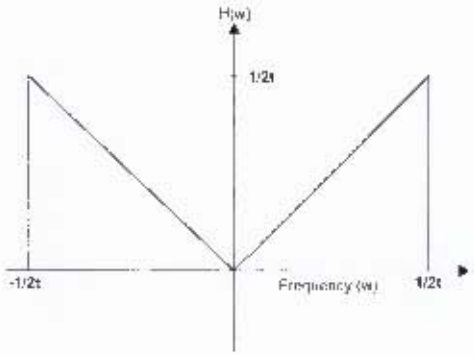

Figure 11: Ideal ramp filter in the frequency domain.

Multiplication in the frequency domain is equivalent to convolution in the spatial domain, making this fast and simple to implement. In order to add each projection's contribution to the final reconstruction, each projection is smeared across the original image space.

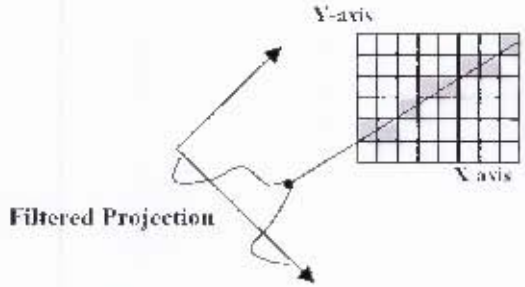

Figure 12: Each point of projection data is smeared across the image space to add its contribution to the final reconstruction.

Thus, for each angle θ the value of t for all points in the projection are back projected along the original summation lines. The filtered back projection contributes the same value of t to each (x, y) pixel along the line. The back projection recreates the original object via the constructive addition of successive overlays of projection data.

We can also see how the quality of the final reconstruction is influenced by the number of scans used in the reconstruction. As the number of scans is reduced the image becomes blurry and fine details are lost. If we remember the Fourier slice theorem we can see how having fewer scans means having less frequency domain data and especially relatively less high frequency data. We are thus trying to approximate an inverse 2D Fourier transform with sub sampled data. Also notice the star artifacts that are common with this type of reconstruction. These are the

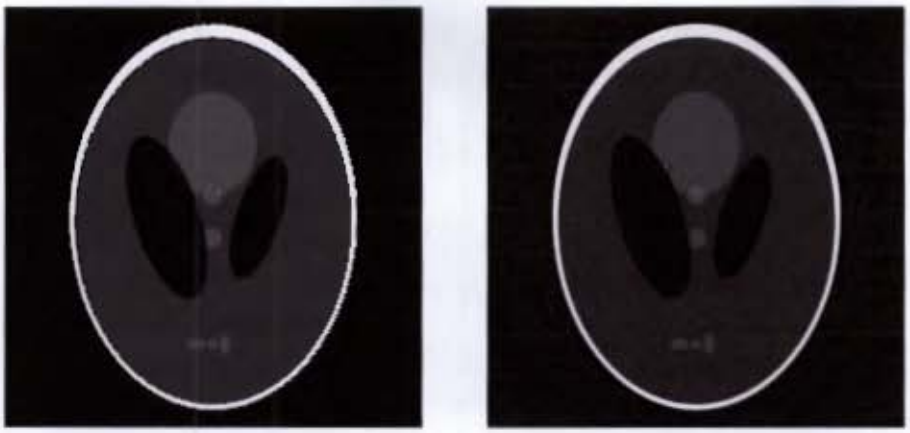

(a) Original head phantom

(b) Backprojected image using scans from 0 to 180 degrees with one degree stepping

Figure 13: Original head phantom and filtered back projected image.

visible remains of the smearing process where each scans data is added to the common image space.

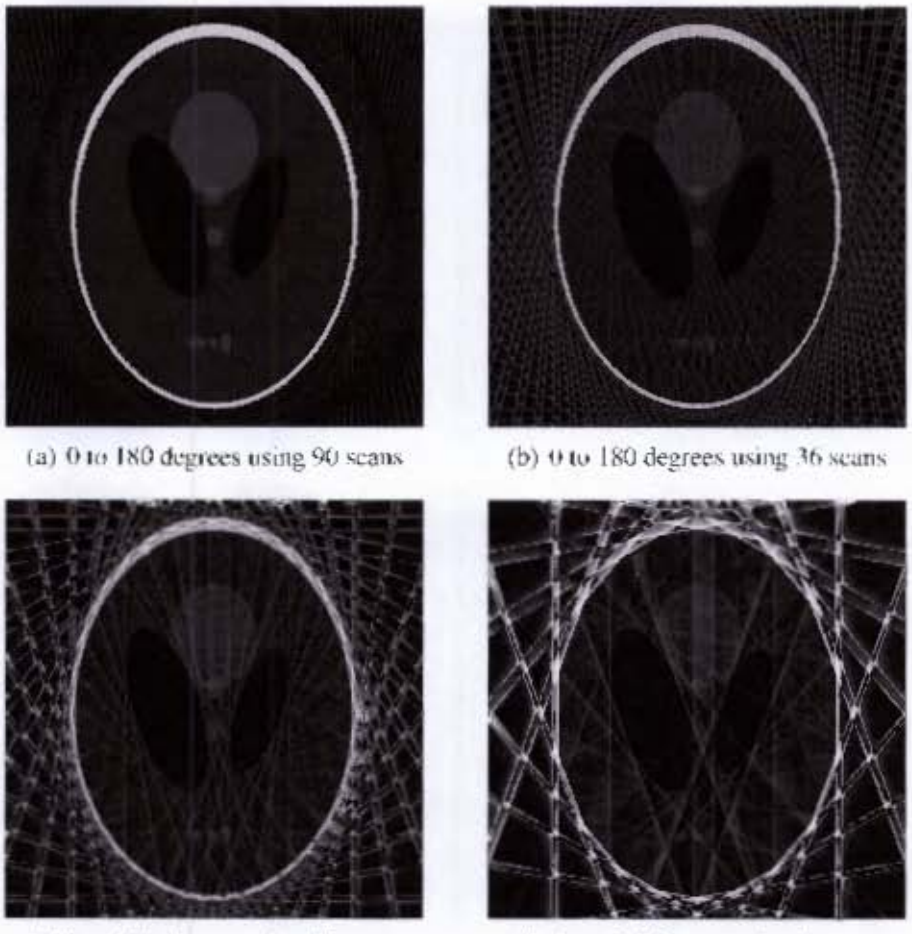

(a) 0 to 180 degrees using 90 scans

(b) 0 to 180 degrees using 36 scans

(c) 0 to 180 degrees using 18 scans

(d) 0 to 180 degrees using 9 scans

Figure 14: Multiple reconstructions of the original head phantom using fewer and fewer scans over the same angular range

We can also see the results of trying to reconstruct the original phantom with scans over a smaller angular range. The reconstruction is distorted as we are missing too much information to perform a proper reconstruction.

Figure 15: Reconstruction of original head phantom using scans from 0° to 90°.

3 X-ray Distortion

In this chapter the general problem of x-ray distortion is discussed as well as the specific problems associated with the LODOX StatScan machine.

3.1 X-Ray Distortion

Traditional x-ray images contain a distortion introduced by the geometric shape of the of the beam of x-rays that passes through the patient before being captured by some suitable photographic device. This makes accurate measurement from the x-rays difficult. While there are procedures to remove this distortion, it remains a non-trivial task.

The most common shapes of x-ray beams are: a cone of x-rays radiating from a point source, or a collimated fan-beam radiating from a point source (seen in figure 16). In the case of the cone-beam, the final image will contain non-linear distortions in multiple axes radiating from the center of the image. In the case of the fan beam, the image will only contain a distortion in the direction of the beam width, but not in the scanning direction of the x-ray image.

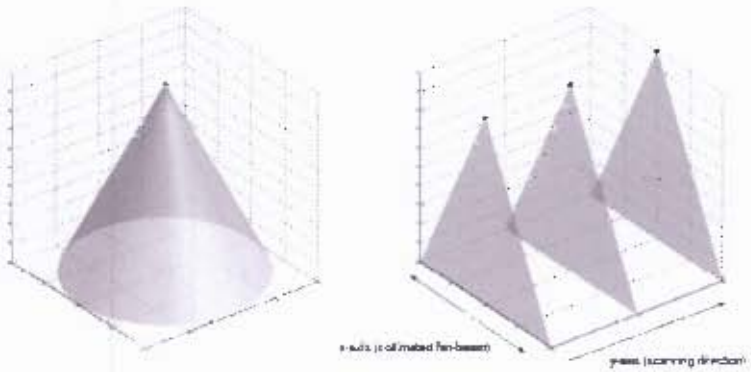

Figure 16: Cone and Fan beam geometries

Internal features will appear distorted depending on their depth and horizontal position relative to the x-ray source and detector due to the divergence of the x-ray beams. Objects near to the center of the spread of the beams will be less distorted than those near the edges where the beam spread is greatest (scaling error). Some internal features might appear to be shifted from their true positions based on the angle of the incident x-rays (positional error).

As can be seen in figure 17, nearer to the center of the spread of x-rays the object will appear less stretched than towards the edge of the fan beam due to increasing beam divergence. In addition to this, note the two structures on the left hand side of the object. The fan x-ray beam passes through both of these structures before reaching the detector. Therefore these structures will appear to be on top of each other in the final image, creating a positional error.

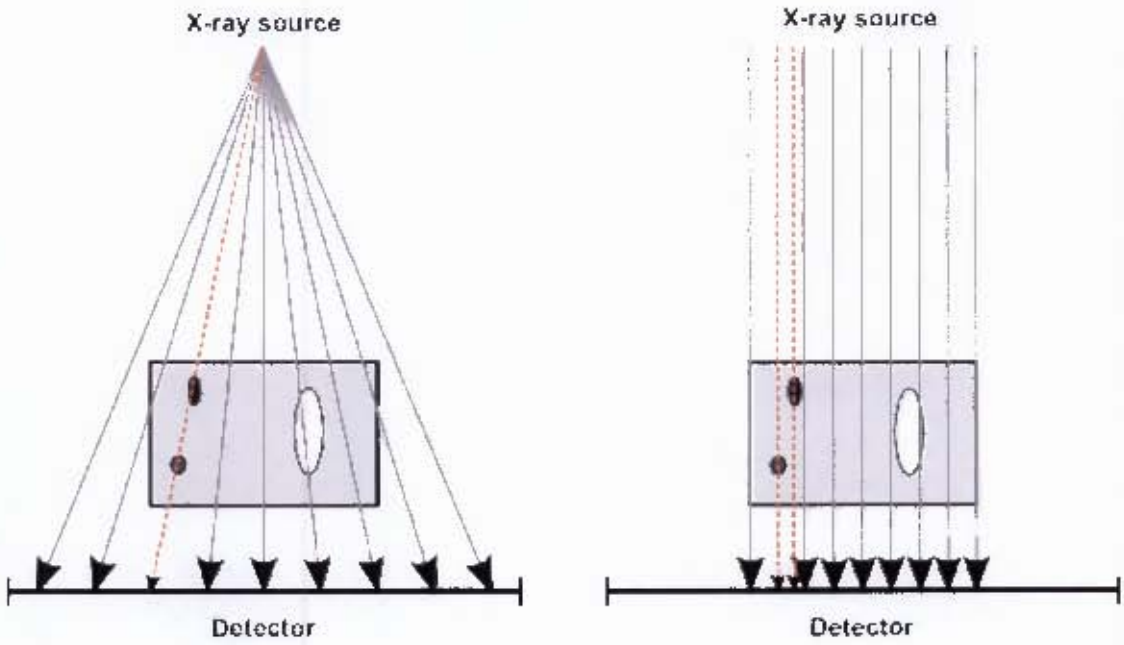

Figure 17: Distortion from beam spread

This is in contrast to the parallel beam example shown where both the scale and relative positions of the object's internal features are preserved. Thus we can see that an x-ray image produced from a parallel beam source would be ideal for the purposes of measurement, requiring no scale correction.

Figure 18: Original fan beam x-ray with positional error of bones highlighted.

We can also see this in a real world example. Here in Figure 18 we can see how the two highlighted bones appear to be behind each other.

However, once we correct for the distortion present in the image due to the spread of the fan beam we can see (Figure 19) that those two bones are not actually directly behind each other. Also note how the knees in the new image appear less stretched horizontally once the spread of the fan beam x-rays are removed.

In figure 20 we can see that if the object is too close to the x-ray source not all of it will be imaged, as it will fall outside of the fan beam of x-rays. The closer it is to the x-ray source the greater the magnification error will be due to the beams divergence.

Figure 19: Corrected x-ray image with true position of bones highlighted.

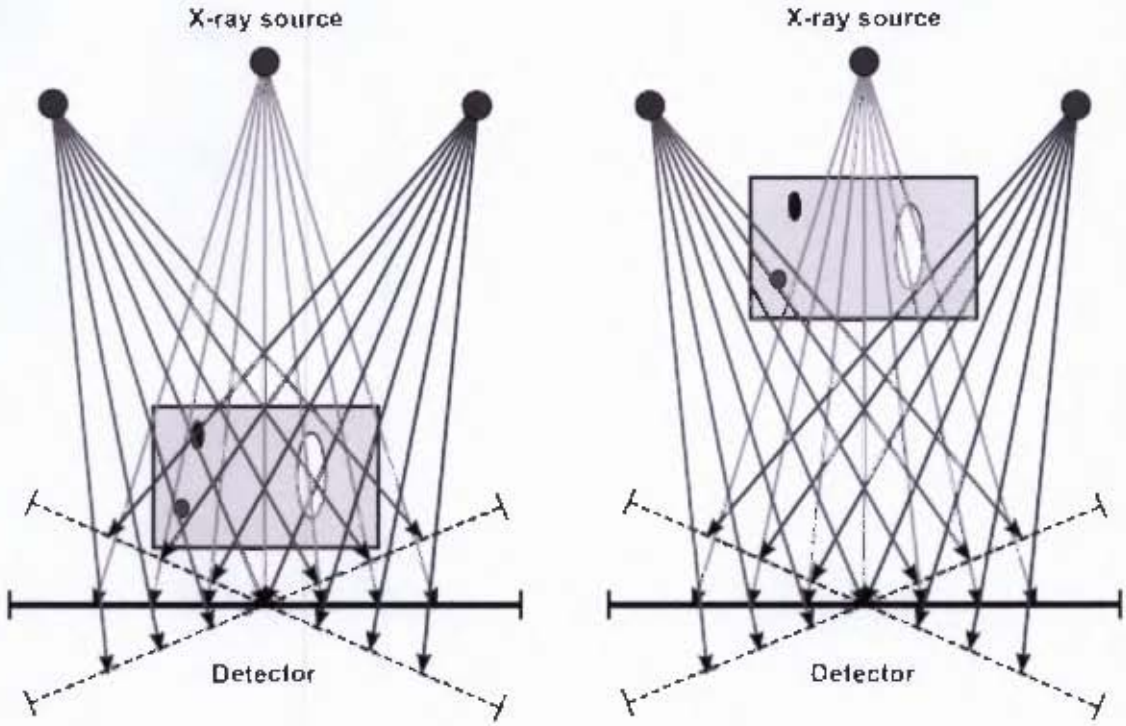

Figure 20: Distortion from height relative to detector

3.2 Correcting For Distortion

There is a need for distortion free x-ray images that would allow internal dimensions to be measured accurately. Current procedures only compensate for scaling errors and not positioning errors of internal features.

The current procedure of taking measurements from an x-ray image involves placing a lead ruler near the area of interest (seen in figure 21). This ruler must be as close to the area of interest as possible so as to be similarly distorted in the final x-ray image. This ruler is then used to calculate the magnification factor of the image. Measurements are multiplied by the magnification factor to attempt to correct for the scaling distortion Markgraaff [2003].

However this method assumes distortion linearity along the length of the ruler. As the ruler moves further from the center of the spread of the x-ray beam it will suffer from the same

Figure 21: Composite of three x-ray images aligned using lead ruler

increasing distortion that the rest of the image suffers from. In addition, if the ruler is not at the same level and orientation as the feature to be measured, further errors are introduced due to the diverging nature of the x-ray beams (eg. an incorrect magnification factor would be calculated).

Current workarounds include trying to keep the area of interest under the center of the x-ray beams (where the divergence is small). This involves taking multiple scans with the object of interest at different horizontal positions. These are then joined together to try to minimize the overall distortion present. This can be seen in Figure 21 where multiple images have been joined to create a composite.

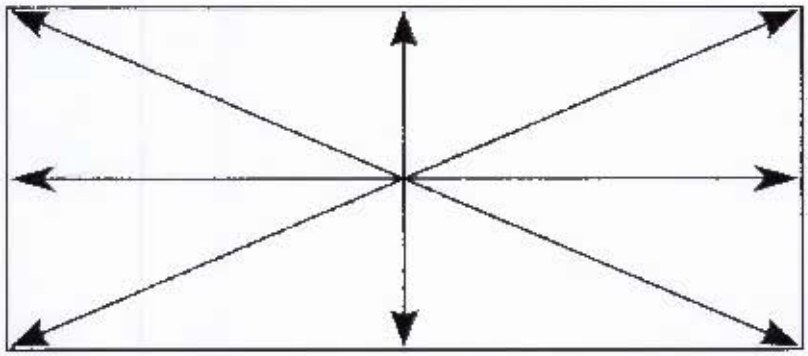

(a) X-ray distortion present in a standard con-beam x-ray image.

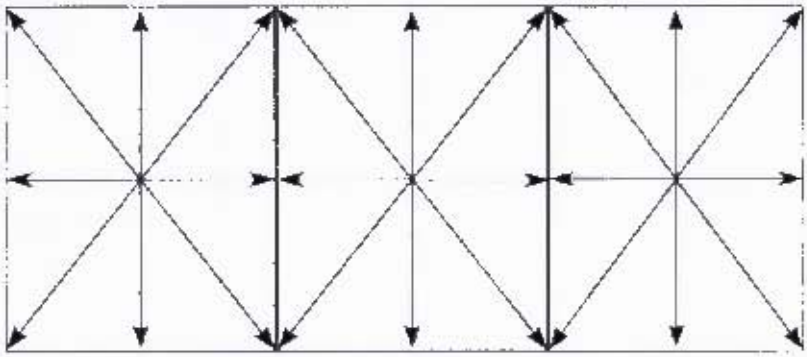

(b) X-ray distortion present in a composite image.

Figure 22: X-ray distortion in both a standard con-beam x-ray and a composite image designed to minimise distortion

However this does not eliminate the problem, it only minimizes it. It also introduces multiple areas of non-linear distortion into the final composite image. There is also no correction for the non-linear distortion of the Y-axis of the image (assuming these images came from a cone beam source). Additionally there is the problem of alignment of the multiple images and possible different exposures between images. It would be better if the entire area could be imaged at the same time to minimise these problems.

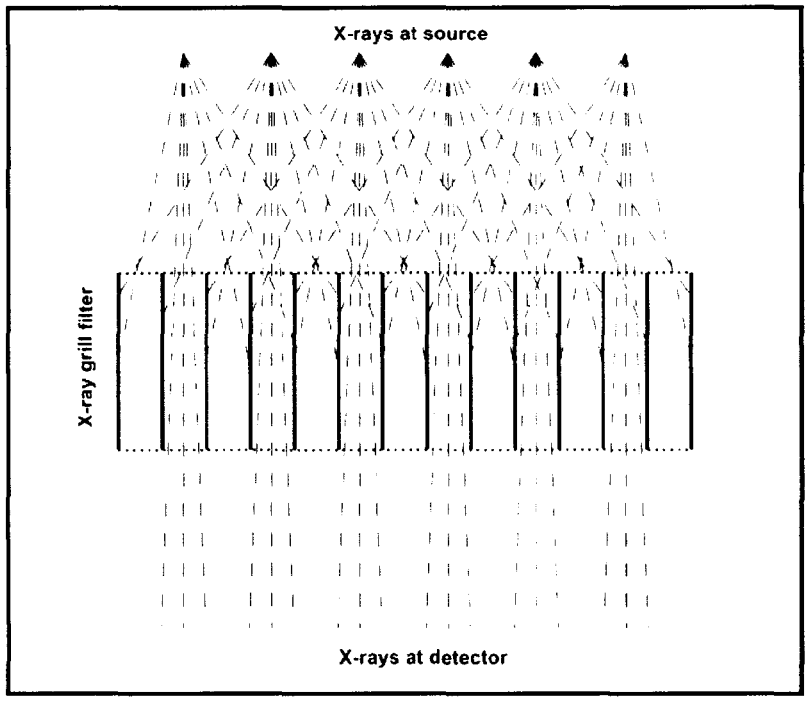

Figure 23: X-ray grate filtering out non-parallel x-ray beams.

An alternate method for correcting for the distortion in the images would be to take the x-ray using parallel beam x-rays. However this is difficult as the x-rays will always tend to radiate out uniformly from the x-ray source. One can select for the 'most parallel' rays using a grate. However while this results in parallel rays (Figure 23) there is a large loss of x-ray power which leads to a loss of resolution in the final image.

With the StatScan machine, the image produced will be geometrically correct in the scanning direction but distorted in the direction of the fan beam spread (perpendicular to scanning direction). Thus there is only one axis of distortion that needs to be corrected. To allow for accurate measurements to be taken, it would be best if the images produced by the StatScan machine's fan beam x-ray could be converted into the equivalent image that would have been produced by parallel beam x-rays. A parallel beam image would show the accurate scaling and position of the internal features of objects.

3.3 The LODOX StatScan Machine

The x-ray images for this thesis were taken using the LODOX (low-dosage x-ray) StatScan experimental scanner at Groote-Schuur hospital. The StatScan machine is a digital x-ray scanner capable of full body imaging of a patient within 13 seconds. It was originally developed by Debex, South Africa, for detecting diamond smuggling amongst mine workers. The technology was adapted for use in the trauma units of hospitals for the quick assessment of internal injuries of patients. An example of one of their machines is seen in figure 24. One of the major benefits of the StatScan machine, to both patients and doctors, is the extremely low radiation dose used in acquiring an image.

Figure 24: LODOX StatScan Machine

The StatScan machine images objects of interest by means of an x-ray tube and detector mounted on opposite sides of a mechanical c-arm. The x-ray source produces a collimated fan shaped beam of x-rays as seen in figure 25. This is in contrast to the cone beam emissions of conventional x-ray units.

These x-rays are detected, at the other end of the c-arm, by a bank of scintillator arrays. These convert the x-rays into visible light. These are in turn optically coupled to charged coupled devices (CCD's) which convert the visible light into digital information. The CCD's are 60um and (when the StatScan collimator is fully open) provide a maximum of 5800 elements along along the detector bank. Spatial resolution is selectable from 1.6 to 4.1 line pairs per millimeter depending on the binning rate of the detector. The detector records 14 bits of gray-scale color information.

To produce an x-ray image the c-arm is moved linearly over the object of interest (Y-axis) with the fan beam of x-rays perpendicular to the direction of motion (X-axis) as seen in figure 26.

The c-arm can be rotated around the object of interest to produce x-ray images at different angles (from 0°to 90°). This provides AP, oblique and lateral imaging. It cannot rotate and take an x-ray at the same time however. It must first be rotationally positioned and then a linear scan can be taken.

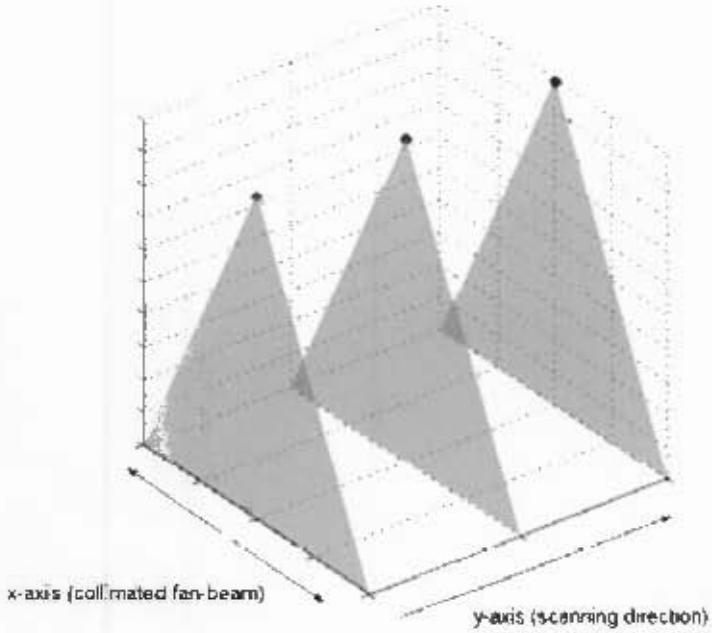

Figure 25: Collimated fan beam of x-rays

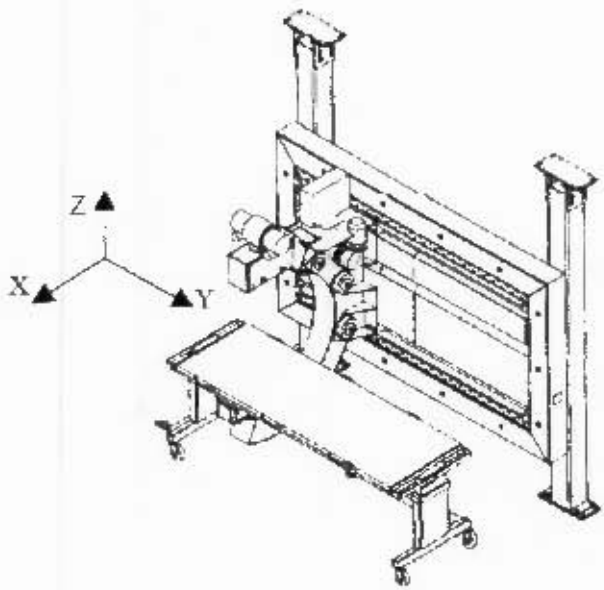

Figure 26: StatScan machine showing principle axes of operation

X-ray images produced by the StatScan machine contain a non-linear distortion in the direction of the spread of the fan beam of x-rays (the X-axis). However the images are accurate in the scanning direction of the c-arm (the Y-axis). Thus in terms of the problem of producing accurate images from the StatScan scans, there is only one axis of distortion to be corrected.

4 Distortion Correction Processing

In this chapter the process of taking raw images acquired from the StatScan machine and correction for their geometric distortion is discussed.

4.1 StatScan Image Acquisition and Geometry Correction

This section shows the process behind how the images taken by the StatScan machine are acquired. The preliminary image processing and geometric corrections needed before using these images in the final fan to parallel beam conversion is also discussed.

4.1.1 Acquiring Scans

For the distortion correction method presented here, multiple fan beam scans at different angles are combined into a single parallel beam scan. Thus a decision must be made as to how many scans are sufficient for an acceptable reconstruction.

Each set of scans is done at one degree increments with the starting and ending angle determined by the width of the object and its horizontal position on the table. Care must be taken to completely include the object being scanned within the beam width of the x-ray.

With the multiple scans we are attempting to have 'parallel' information covering the whole object. This can be seen if we imagine that the detector is fixed and the x-ray source can rotate freely above it. Because of the nature of the diverging fan beam of x-rays, for each scan some of these rays will strike the detector at 90° .

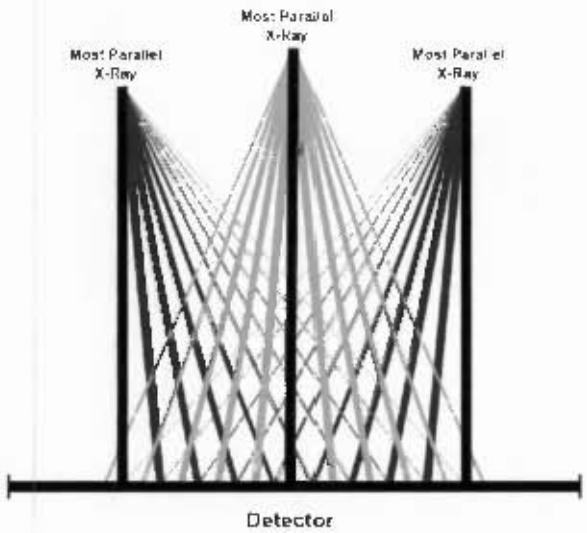

Figure 27: `Most parallel` rays from each angular increment.

It is not required to have a parallel ray strike the detector for every section of the object being imaged. That would require an unfeasible number of scans and would expose any patients to

unacceptable amounts of radiation. Instead it is sufficient to take scans at one degree rotational increments that provide parallel information from one edge of the object to the other.

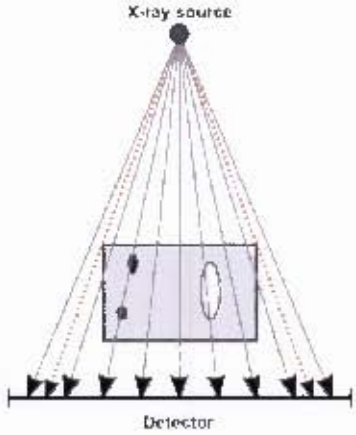

Figure 28: Object width determines fan-out angle of x-ray beam.

The size of the object being scanned determines the fan-out angle of the x-ray fan beam and from this the angular range of scans needed to provide parallel information from edge to edge. For example, if the object width means that the fan-out angle is 20° then you would require a set of scans covering from -20° to $+20^{\circ}$ from the central scan of the object. This would ensure parallel x-ray information for the entire width of the object being scanned.

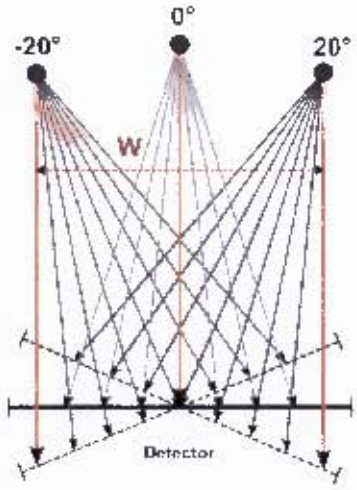

Figure 29: Maximum width of object with a 20° fan-out angle

Once these scans have been acquired they first have to be aligned relative to each other before the distortion correction algorithm can be applied. This is due to the StatScan machine's C-arm not starting and stopping at the same linear position for each scan at different rotational positions. While it possesses very accurate position sensing both linearly and rotationally, it was not designed with the need to accurately repeat a series of scans from the exact same positions every time. Thus when positioning the c-arm there is a tendency to overshoot the mark.

4.1.2 Preliminary Image Processing

Certain preliminary image processing stages are needed before the scans from the StatScan machine can be used to create a distortion free image (de Villiers [1999a]).

- Vertical Alignment: All of the x-ray images must first be aligned in the scanning direction. The machine has a very accurate linear positional sensor but does not always start scanning at the specified position. A marker was used to define the start position of all images. This marker is detected by the software and used to align the images without the need for more complex image registration techniques. This is done using basic edge detection. A general range is defined to search for the marker within the image. The software finds the point of discontinuity where the image intensity changes from background to the beginning of the marker. This position is then set as the top of the image.
- Background Removal: The table which supports all scanned objects is designed to be as transparent to x-rays as possible while still retaining sufficient strength. It is approximately uniform in the scanning direction and thus subtracting an expected amount from all rows in the image is a simple task. The profile of the table is built by taking an average of the rows in the image where only the table is present. This is useful for an extension to the distortion correction procedure (see Chapter 5) which involves a partial back projection and where the table could introduce unwanted noise into the reconstructed image.
- Horizontal Binning: It may be necessary to create a lower resolution data set for testing purposes. This can be done by reducing the horizontal resolution of the images. This can help to speed up the processing stages of the distortion correction algorithm.

4.1.3 Off Center Correction

The mechanical center of rotation of the StatScan machines c-arm does not fall on the mid-line of the fan beam of x-rays radiating from its x-ray source (figure 30). For calculation purposes, the ideal fan beam geometry occurs when the mid line of the fan beam passes through this center of rotation and the distance from the source to the center of rotation is equal to the distance from the center of rotation to the detector (Crawford et al. [1988]).

The images taken by the StatScan machine must be corrected to compensate for the physical geometry of the machine's source-detector pair (de Villiers [2003]) (the c-arm seen in figure 26). If this is not changed then all subsequent calculations are unnecessarily complicated.

A reprojection of the x-ray data onto a new virtual detector is created. This virtual detector plane has the mid line of the fan beam of x-rays passing through the physical center of rotation of the system (figure 31).

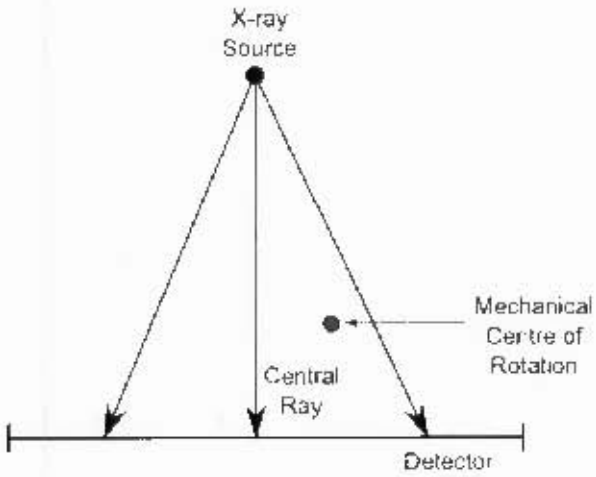

Figure 30: Mechanical center of rotation relative to StatScan machines source and detector pair

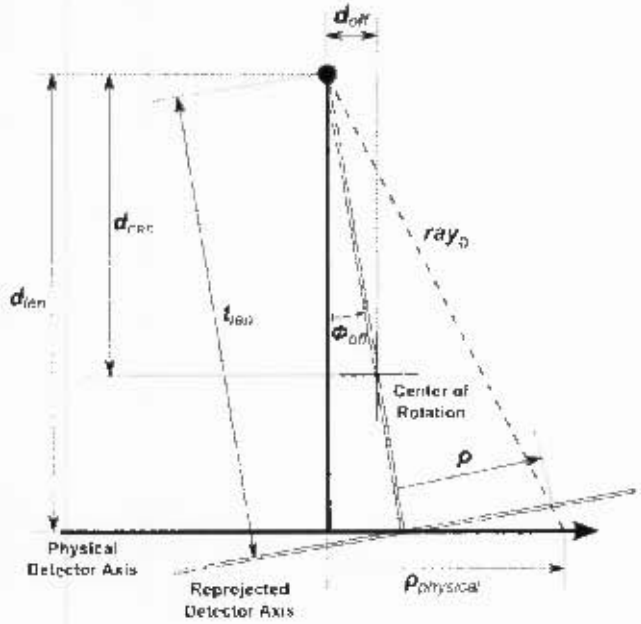

Figure 31: Original detector axis vs reprojected detector detector axis

For continuous projection axes ρ and $\rho_{physical}$, the projection values are preserved such that

$$P(\rho) = P_{physical}(\rho_{physical}), \tag{7}$$

where

$$\rho = t_{len} \tan\left(\tan^{-1}\left(\frac{\rho_{physical}}{d_{len}}\right) - \phi_{off}\right) \tag{8}$$

$$\phi_{off} = \tan^{-1}\left(\frac{d_{off}}{d_{cen}}\right) \tag{9}$$

$$t_{len} = \frac{d_{len}}{d_{cen}} \sqrt{d_{cen}^2 + d_{off}^2} \,. \tag{10}$$

However the projection axes are not continuous and so in the practical implementation linear interpolation is used for the discrete case:

$$(\lceil \rho \rceil - \rho) P(\lfloor \rho \rfloor) + (\rho - \lfloor \rho \rfloor) P(\lceil \rho \rceil) \approx P_{physical}(\rho_{physical}) \,.$$

On the physical detector axis discrete measurements are limited by the size of the CCD devices and the properties of the scintillator array (which converts the x-rays to visible light). The CCD's are 60um and (when the StatScan collimator is fully open) provide a maximum of 5800 elements along the detector bank. Spatial resolution is selectable from 1.6 to 4.1 line pairs per millimeter depending on the binning rate of the detector. A higher resolution image also introduces a larger amount of noise into the final image.

The physical measurements d_{len}, d_{cen}, and d_{off} can be obtained by taking of scans of a reference object from a range of angles and combining markings on the object with their visible projections in the image. These measurements were made by Mattieu de Villiers on the StatScan machine used in this research de Villiers [2000a]. From these values all others can be derived:

$$d_{len} = 1299mm, \quad d_{cen} = 954.55mm, \quad d_{off} = 60.23mm \,.$$

Knowing the physical detector size is 60um and the binning rate for the image, allows us to convert these measurements into pixel distances:

$$Pixel\ Distance = \frac{Machine\ Measurement}{Detector\ Size \times Binning\ Rate} \tag{11}$$

Figure 32: Original scan taken by StatScan machine

In figure 32 we can see an original scan taken by the StatScan machine.

Figure 33: Center of rotation corrected image

In figure 33 we can see the same scan once it has been corrected for the off center of rotation. This is equivalent to a shift of the data horizontally. This is repeated for every scan taken at every angle.

This corrected projection data can now be used in the next phase of the distortion correction method, namely converting from fan beam data to parallel beam data.

4.2 Fan to Parallel Beam Conversion

This section shows how the corrected StatScan images have their fan beam data rebinned into parallel beam data. Once the data has been corrected for the off center of rotation it is then suitable for conversion to parallel beam data. This is accomplished by referring the fan beam projection axis to a new projection axis which passes through the center of rotation. From this the data is rebinned into a virtual parallel beam axis using information from multiple fan beam scans.

4.2.1 Fan Beam Rebinning

A common x-ray beam geometry is that of a fan beam. This causes distortion in the direction of the spread of the beam. An ideal beam geometry for the purposes of measurement would be that of a parallel beam x-ray (Kak and Slaney [1988]).

So, from figure 34 we can see that in order to create our parallel beam projection axis $\rho^{\|}$, it would be useful to first refer our original fan beam projection axis ρ to a virtual fan beam axis $\rho^{'}$ which passes through the center of rotation. We assume equal projection values at any point on the axes intersected by the same x-ray, i.e.

$$P_{\phi}(\rho) = P_{\phi}^{'}\left(\rho^{'}\right) = P_{\phi k}^{\|}\left(\rho^{\|}\right) \tag{12}$$

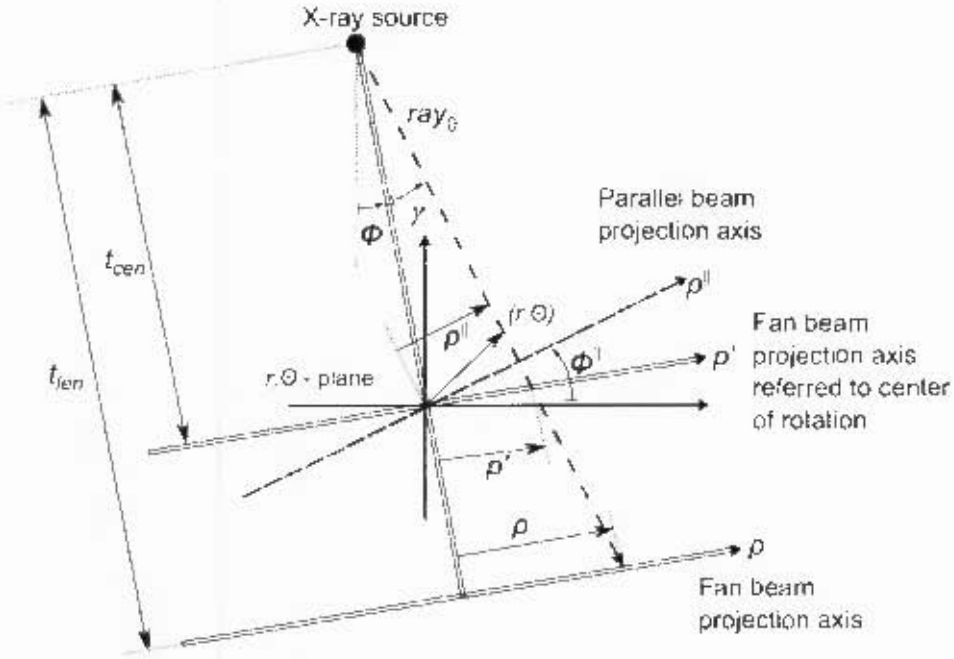

Figure 34: Parallel beam rebinning

We can see that we can extract our parallel beam projection data from the fan beam data. In order to create one parallel beam image at angle $\phi^{\perp}$, we need multiple fan beam images at different angles of ϕ. Then we can use the following equations to extract the parallel data,

$$\rho^{\perp} = \rho' \cos\gamma = \frac{\rho' t_{cen}}{\sqrt{\rho'^2 + t_{cen}^2}} \tag{13}$$

$$\rho' = \rho \frac{t_{cen}}{t_{len}} \tag{14}$$

$$\phi^{\parallel} = \phi + \gamma \tag{15}$$

$$\gamma = \tan^{-1} \frac{\rho'}{t_{cen}} \tag{16}$$

Thus from multiple fan-beam scans, a single equivalent parallel beam scan at angle $\phi^{\parallel}$ can be created.

4.2.2 Creating Sinogram From Available Scans

A sinogram is a representation of projection data over an angular range. We take the multiple fan beam scans from the StatScan machine and combine their information into multiple sinograms, one sinogram for each line in our image. It is on these sinograms that we will perform the fan to parallel beam conversion using the equations defined in the previous chapter.

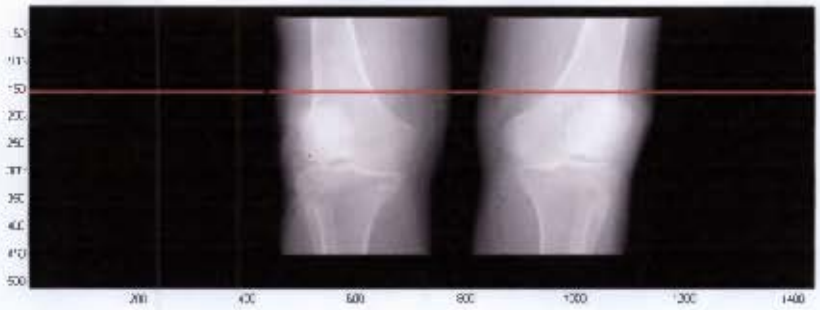

Figure 35: Knee at 2 degrees

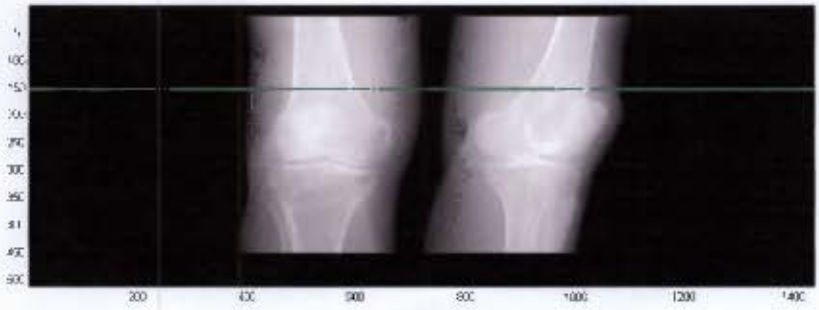

Figure 36: Knee at 20 degrees

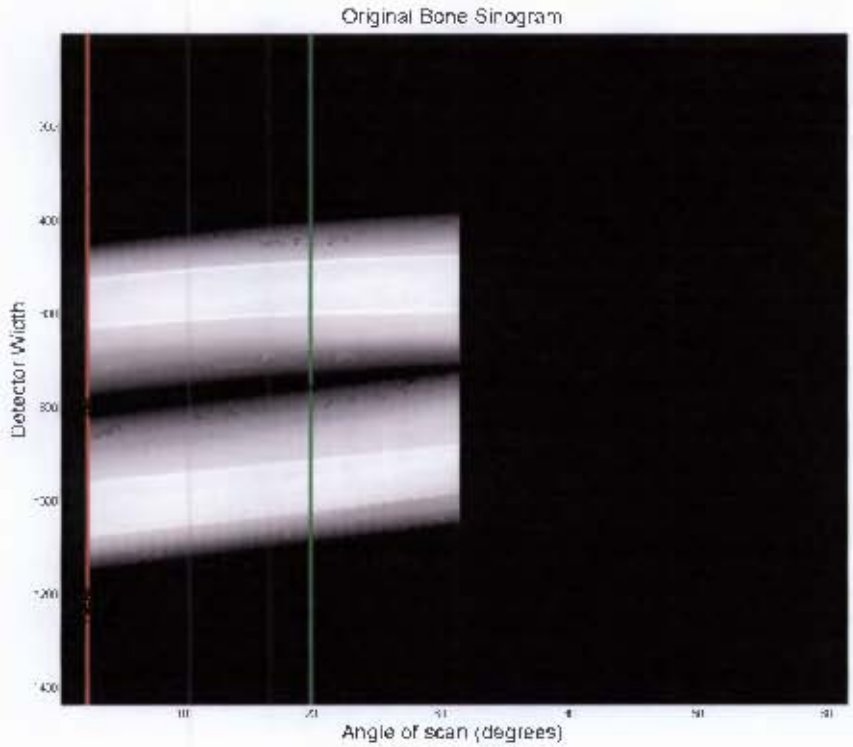

Figure 37: Sinogram constructed from knee scans with lines at corresponding angles highlighted.

From this the fan beam sinogram data is rebinned into parallel beam sinogram data. This new sinogram can be seen in Figure 38.

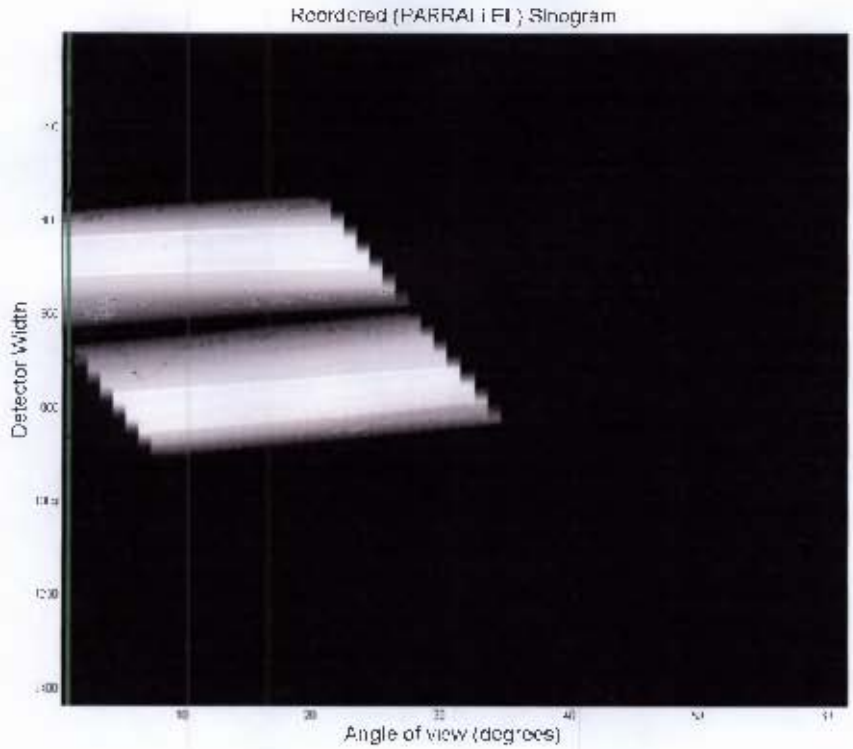

Figure 38: Rebinned sinogram data with selected angle for final image.

From this we select the angular view that we wish to have parallel information on and use it to construct a line in our final parallel beam image (Figure 39. This process is repeated for every line in the image being reconstructed.

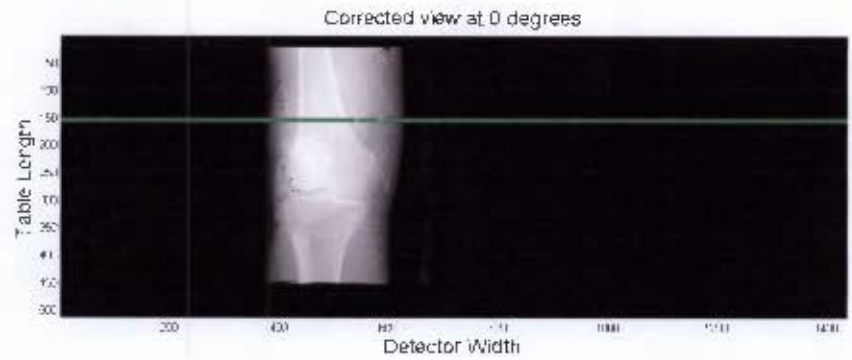

Figure 39: Parallel beam corrected image with line from corrected sinogram highlighted.

4.3 Scale Correction

In this section the final process of taking measurements from our corrected images is discussed.

4.3.1 Scale Correction

Once the fan beam projection data has been rebinned into parallel beam data, measurements can be taken directly from the image data. However the pixel distance measurements must be corrected for based on the binning rate of the image in order to get real world distances. Knowing that the CCD sensor size is 60um and the binning rate allows us to use the following,

$$Pixel\ Distance \times (Detector\ Size \times Binning\ Rate) = Corrected\ Measurement \quad (17)$$

Using this measurements can be taken directly from the corrected images.

5 Reducing Scans Using Back Projection

In this chapter a method for reducing the required number of scans for a distortion corrected image is introduced.

5.1 Limited And Sparse Angle Tomography

If we consider the process of producing a distortion corrected x-ray image we can see that the basic stages are:

- Acquire scans at one degree increments
- Correct for StatScan geometry
- Rebin fan beam information into parallel beam information
- Use parallel beam information to build corrected image

This works well when sufficient initial scans have been taken. However if scans were taken every 2° and the same correction procedure applied then the final result is seen in Figure 40.

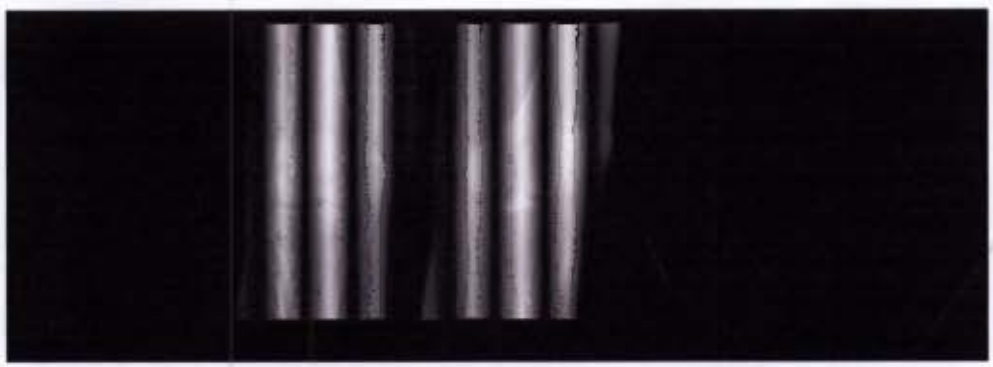

Figure 40: Distortion corrected image using scans with 2° spacing.

Here large gaps can be seen in the corrected image. This is due to missing information in the sinogram from which this image is reconstructed. What is needed is a method to fill in those gaps to allow for a proper reconstruction. If we consider the problem of reconstructing a slice of a head phantom using sparse angle tomography and filtered back projection we can see that we do not need a scan at every angle to produce a good quality final image. Missing information is filled in through the layering and smearing process of the back projection.

Consider our head phantom and the sinogram produced by taking evenly spaced scans at 2° intervals.

Now we see the result of back projecting this sinogram to attempt to produce the original head phantom.

(a) Original head phantom

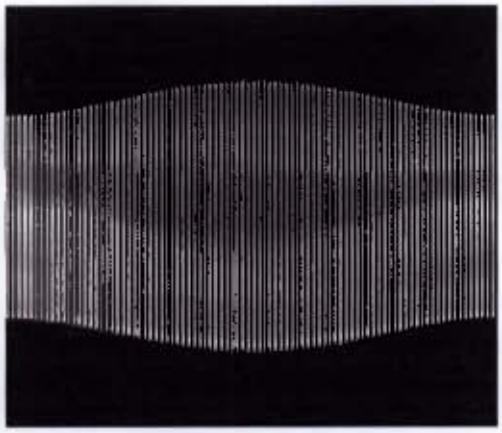

(b) Sinogram over 180 degrees with 2 degree stepping

Figure 41: Using filtered back projection with sparse angle tomography

Figure 42: Reconstruction of original head phantom using sparse angle back projection.

But what would the sinogram of this reconstructed image look like compared to the full sinogram data of the original head phantom?

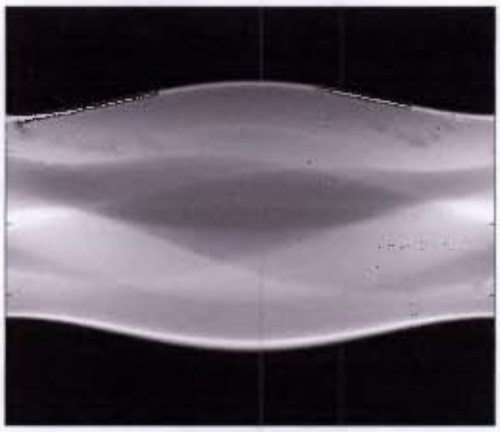

(a) Original sinogram of head phantom

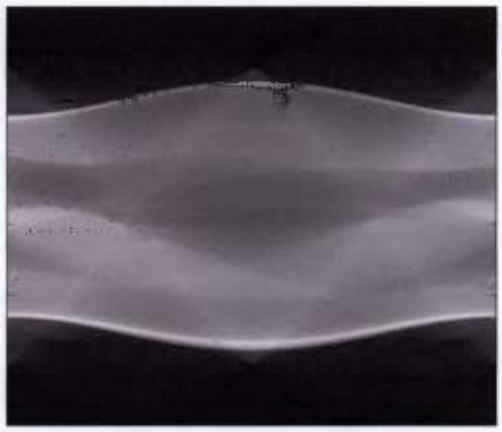

(b) Sinogram data from reconstructed image

Figure 43: Comparison of sinogram data of original head phantom vs sinogram data from the reconstruction

From this we can see that the back projection process has filled in the blanks present the sinogram in Figure 41. We can accomplish a similar smoothing of the sinogram data without needing a full slice reconstruction.

6 Implementation

In this chapter the implementation of the distortion correction method is discussed. A flowchart (Figure 44) of the different stages of processing a LODOX image is presented as reference.

6.1 Capture Data

Capturing data using the LODOX StatScan machine is an entirely manual process. An initial exploratory scan is performed to determine the power and binning required to produce acceptable image quality. This also helps to determine how many scans will be required to produce a corrected final image. The C-Arm rotation must be set manually for each scan. Time must be allowed for the StatScan machine to cool down between each series of scans to prevent the x-ray tube from overheating. Each image must then be exported individually from the local format to the Dicom image format. These can then be manipulated by Matlab (the language in which the bulk of the processing is performed).

6.2 Image Preprocessing

With the x-rays exported into Dicom images some preliminary processing must be done to compensate for some problems with the StatScan machine. The images must be vertically aligned as the C-Arm does not begin scanning from exactly the same point every time. This is performed using simple edge detection on the x-ray image with some suitable dense object (a pin or metal ruler) providing a reference.

6.2.1 Off Centre Correction

After the images are aligned they are now suitable for the off centre correction. However in practice, and to reduce errors from multiple linear interpolations, this stage and the rebinning stage are performed at the same time.

6.3 Convert To Parallel

This is where each fan beam x-ray has its data rebinned into an equivalent parallel beam image. This is performed by, for each line of the multiple fan beam x-rays, constructing a sinogram. This then is suitable for the rebinning equations discussed in Chapter 4. However in practice this stage is combined with the off centre correction to save on processing time and reduce errors from rounding (Press [1999]).

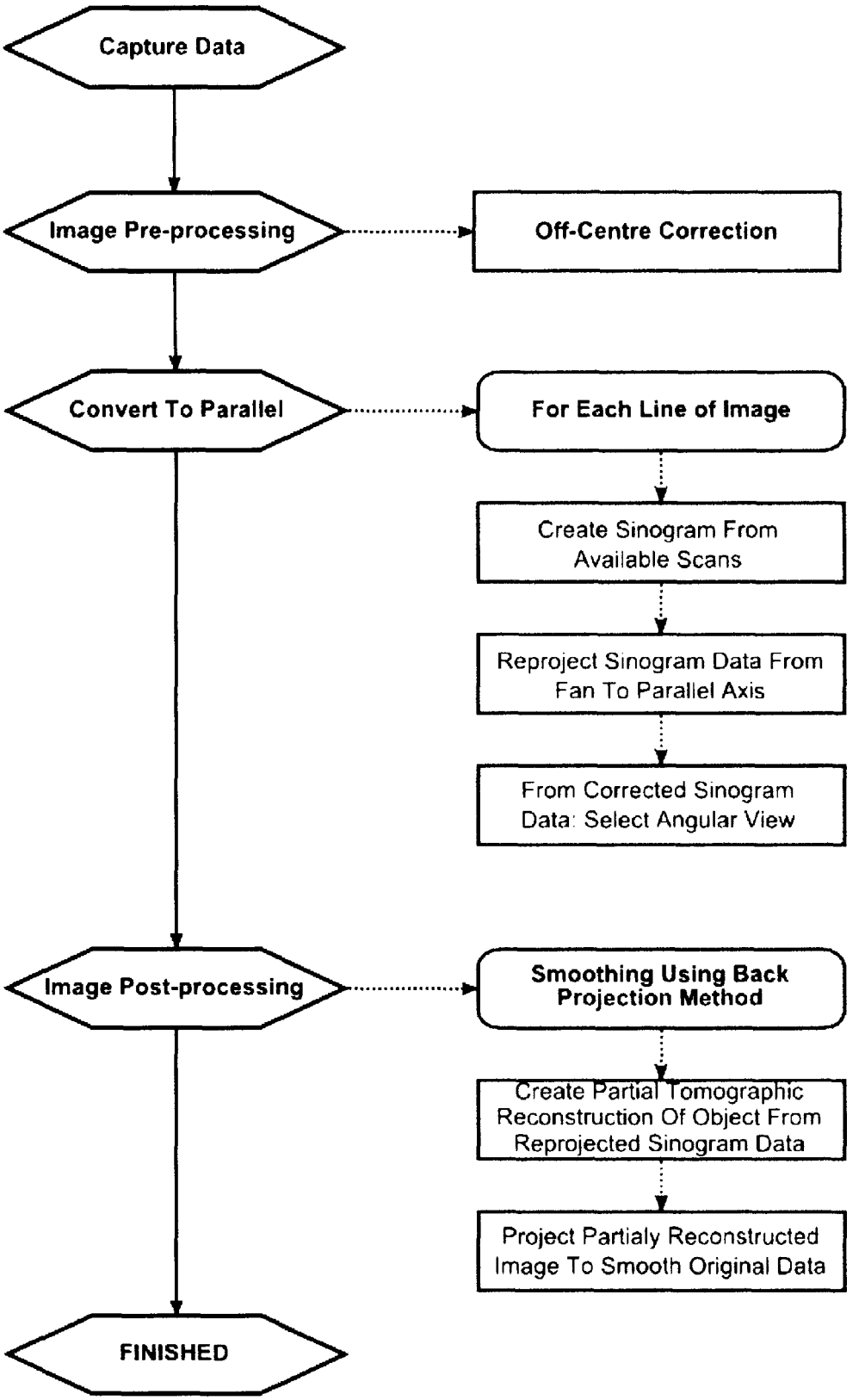

Figure 44: Flowchart of Implementation Steps.

We can see from Figure 31 and 34 that the reprojected detector axis created by our off centre correction is equivalent to our fan beam projection axis used in the rebinning. Through this we can refer our original values on our physical detector axis to our final result on the parallel

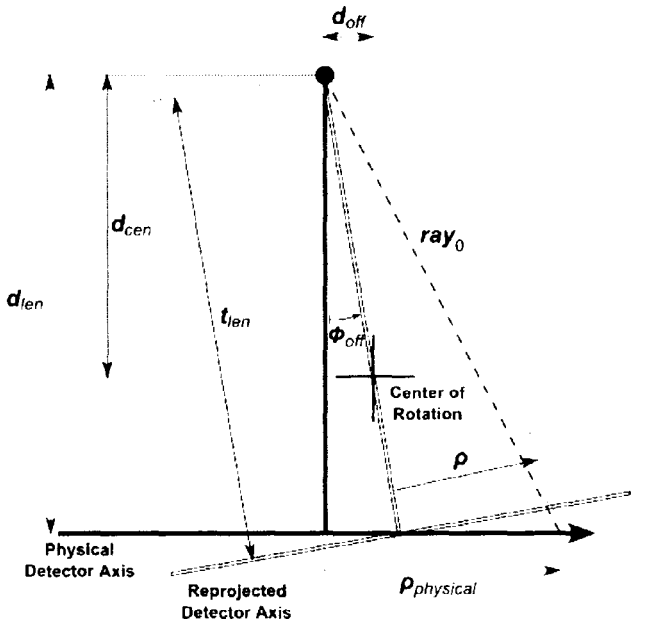

(a) Referring the original scan axis to a new one to compensate for the offset centre of rotation

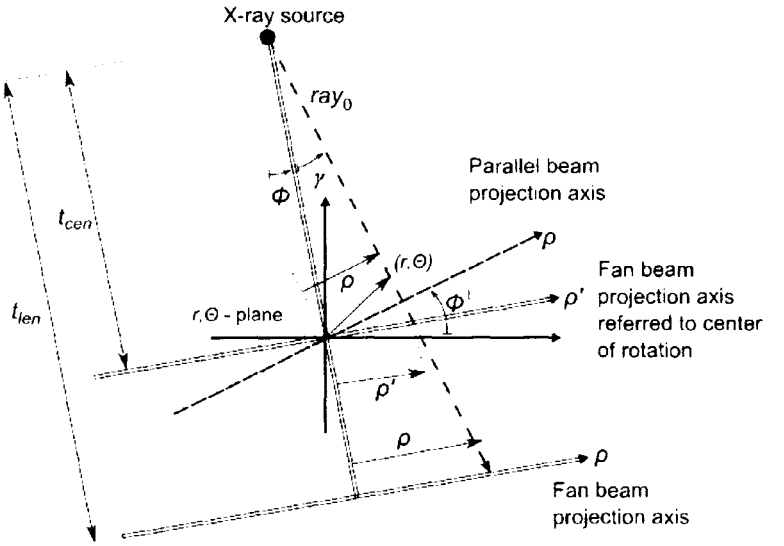

(b) Centre of rotation corrected axis being rebinned into parallel beam axis

Figure 45: Centre of rotation correction and image rebinning.

beam projection axis.

Thus if

$$\rho = t_{len} \tan\left(\tan^{-1}\left(\frac{\rho_{physical}}{d_{len}}\right) - \phi_{off}\right)$$

and

$$\rho' = \rho \frac{t_{cen}}{t_{len}}$$

and

$$\rho^{\parallel} = \rho' \cos\gamma$$

then

$$\rho^{\parallel} = t_{cen} \cos\gamma \tan\left(\tan^{-1}\left(\frac{\rho_{physical}}{d_{len}}\right) - \phi_{off}\right) . \tag{18}$$

This allows us to only have one processing stage and eliminate some unneeded linear interpolation. Using this formula the corrected image is built up from multiple fan beam x-rays.

6.4 Image Postprocessing

Because we may have been limited in the number of scans we could take, or having some of the scans turn out to be unusable, it may be necessary to perform post processing on the final corrected image. This is performed by smoothing using partial back projection methods to reduce the noise in the final image.

7 Results

In this chapter various results are discussed. These demonstrate the accuracy of the distortion correction method as well as their application to live patients.

7.1 Calibrated Metal Blocks

This section demonstrates how accurate measurements can be taken once the image has been rebinned and the horizontal scale of the images is adjusted for according to the binning rate of the images.

These x-rays were taken of accurately machined metal blocks with a 25mm X 25mm base.

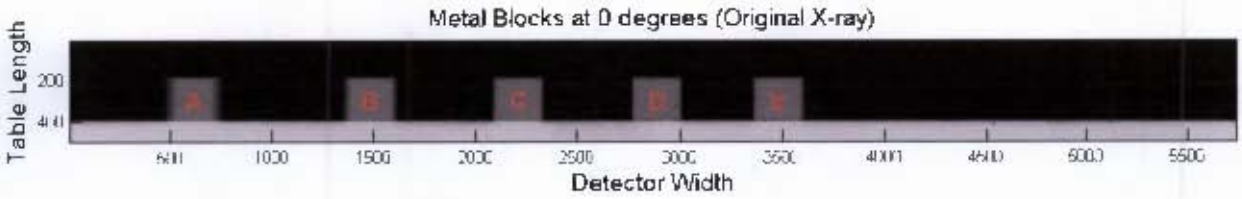

Figure 46: X-ray image of calibrated metal blocks taken at 0° rotation

Multiple x-rays of these blocks are taken and then combined to form an undistorted image at the same angular view.

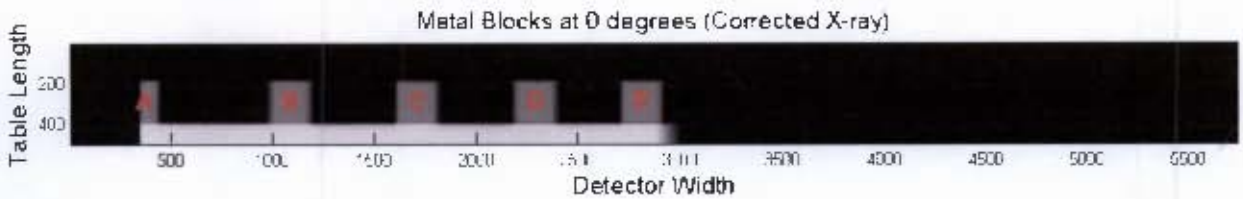

Figure 47: Corrected image of calibrated metal blocks at 0° rotation

Note how the blocks are less stretched horizontally than in the original image. Processing time for 20 x-rays over 500 vertical rows with a horizontal resolution of 5739 was approximately 2 minutes and 21 seconds.

	Original	Error(mm)	Error(%)	Corrected	Error(mm)	Error(%)
A	34.44	9.44	37.76			
B	31.8	6.8	27.2	26.4	1.4	5.6
C	29.88	4.88	19.52	25.6	0.8	3.2
D	28.68	3.68	14.72	26.52	1.52	6.08
E	30.12	5.12	20.48	25.08	0.08	0.32

Table 1: Measurements of calibrated blocks

The measurements in table 1 show clearly the improvements possible with the distortion correction method. In the original scan we can see how the blocks (with D in the center of the table) become more distorted as they move away from the centre of the table. The further from the centre they are the larger the distortion from the beam spread in the width of the table.

In the corrected image we see that insufficient data was available to correct for block A at this angle. However measurements of the remaining blocks shows that their distortion does not increase with their distance from the beams' centre and that their measurements much more closely resembles the expected 25mm of the original blocks.

Of interest is the fact that in both sets of scans the height of the blocks remains the same. This is expected as the StatScan machine is accurate in the scanning direction (table length) and only distorts in the table width axis.

7.2 Cadaver Study

This shows how detail is preserved and an example of how positional errors are corrected for.

Figure 48: Cadaver knee at 2°

The corrected knee shows how errors of placement of internal features are corrected for. The fibula highlighted by the circle can be seen in its true position relative to the tibia in the corrected image.

Figure 49: Cadaver knee at 0°

Note how the other leg could not be corrected for as scans could not be taken from 0 to negative rotations due to limitations of the c-arm of the LODOX machine. This means that not enough parallel information exists for the other leg to be displayed in this view. Processing time for 30 x-rays over 512 vertical rows with a horizontal resolution of 1435 was approximately 41 seconds.

7.3 Live Patient Study

This shows how movement during the scan can compromise the final image quality by introducing large discontinuities. This is obviously in contrast to the cadaver study.

Figure 50: Live patients knee at 0°

When we try to combine multiple images we can see large discontinuities appear due to the patients leg having shifted during the scanning process. This is due in part to the time taken to acquire the needed data for a full reconstruction. It takes approximately 13 seconds for a

full body scan on the StatScan machine and proportionately less time for any small section to be imaged. The C-arm then has to be rotated and repositioned horizontally for the next set of scans. During this time it becomes increasingly likely that the patient will have moved, either himself or through the table being rocked by the motion of the scanning arm. While it is possible to compensate for any purely vertical or horizontal movement of the patient, any rotation cannot so easily be adjusted for.

As an example, if the patients leg rotates by 1° in the same direction as the C-arm is being rotated, from the scanners point of view the leg will not have turned and it would be equivalent to having made two scans at the original orientation. Thus, when using these scans to produce the final image you would be expecting a series of successive rotations that followed 0° ,1° ,2° ,3° ,etc but due to the leg having turned you might have an effective series of rotations of 0° ,1° ,1° ,3° , etc.

The compensation for this could be achieved through a series of markers that would allow pose estimation of the subject in each scan from which the legs orientation could be calculated and adjusted for. Until this is achieved it is best to take as few scans, of the smallest relevant area as quickly as possible to reduce the risk of the patient having moved.

Figure 51: Corrected image of live patients knee at 0°

These discontinuities are especially visible at the edges of the bones and in the metal pins inserted into his knee. Thus we can see the the patient needs to be fully immobilised during scanning or the procedure needs to be significantly sped up. The scale of this image is 5pixels to 1mm. Processing time for 30 x-rays over 931 vertical rows with a horizontal resolution of 2845 was approximately 2 minutes and 9 seconds.

8 Conclusions

It was successfully shown that an undistorted x-ray image could be obtained from scans taken by the LODOX StatScan machine. A Software system was developed and implemented, primarily in Matlab, that took as input multiple StatScan x-ray images and produced as output a single undistorted x-ray image suitable for diagnosis.

The new image is geometrically accurate in both the beam width and scanning direction. This was shown using a test performed with calibrated metal blocks and comparing the measurements in the undistorted image with their known dimensions.

The distortion correction implementation is sufficiently fast to be used in diagnosis. The image processing is performed offline with corrected images available in minutes.

Limitations of the system were exposed during a trial on a live patient. While vertical and horizontal motions can be corrected for in the image preprocessing stages, rotational movement of the object under study cannot. Uncorrected, this causes visible and undesirable discontinuities in the final image that make it impossible to use for diagnostic purposes.

The problem is that the scanner has no way to know the orientation of the patient. If the patient turns in sync with the rotation of the C-arm, to the scanner it would appear as if the patient is not moving at all. Then for every scan there may be some extra positive or negative rotation that may have been introduced by the patients movement. When trying to correct the final scan without knowing absolutely what angle each scan was taken at, shearing errors are created as the wrong parallel information is used to create the final reconstructed image.

The distortion correction method presented here is suitable for use on areas which can be completely immobilised. It is not suitable for the correction of areas containing constant motion such as the chest or internal organs.

The targets of this thesis were met successfully and to the satisfaction of those concerned.

9 Recommendations And Future Work

A method for compensating for the rotational movement of limbs needs to be developed before this can be used on live patients. This could possibly be done using a system of fixed markers which would identify the limbs position in space in each x-ray image.

The StatScan machine needs to be able to automatically handle multiple scans at different angles. The current manual procedure is laborious and time consuming. This is undesirable especially with a live patient as it detracts from patient comfort and increases the risk of movement artifacts being introduced into the final image.

For further increases in processing speed the system could be implemented to take advantage of multiple processing units as it is highly parallel in nature. There would be a near linear speed increase for every additional processor used in the calculations.

To reduce x-ray exposure even further a mechanical system could be integrated into the StatScans collimator that would only illuminate the area of interest with x-rays for each scan.

References

J. L. Ball and A. D. Moore. *Essential Physics for Radiographers, 2nd ed.* Blackwell Scientific, 1992.

R. N. Bracewell. *Two Dimensional Imaging.* Prentice Hall International Inc., 1995.

C. R. Crawford, G. T. Gullberg, and B. M. W. Tsui. Reconstruction for fan beam with angular displaced center of rotation. *Medical Physics*, 15:67–71, 1988.

M. de Villiers. Investigation into the removal of lodox artifacts. Technical report, Digital Image Processing, University of Cape Town, 1999a.

M. de Villiers. Limited angle tomography iii. Technical report, Digital Image Processing, University of Cape Town, 1999b.

M. de Villiers. Limited angle tomography. Master's thesis, University of Cape Town, 2000a.

M. de Villiers. Tomographic angular range of lodox and the consequence of the lateral offset. Technical report, Digital Image Processing, University of Cape Town, 2000b.

M. de Villiers. *Limited Angle Tomography using Lodox.* PhD thesis, University of Cape Town, 2003.

S. Helgason. *The Radon Transform.* Birkhauser, Boston, 1980.

A. C. Kak and M. Slaney. *Principles of Computerised Tomographic Imaging.* IEEE Press, 1988.

H. L. Loats and H. H. Holcomb. *Image Analysis. In: Innovations in Diagnostic Radiology.* Springer-Verlag, New York, 1989.

C. G. Markgraaff. Magnification error correction in statscan images, 2003.

F. Natterer. *The Mathematics of Computed Tomography.* John Miley & Sons Ltd., 1986.

W. H. Press. *Numerical Recipes in C: The Art Of Scientific Computing. 2nd ed.* Cambridge University Press, 1999.

M. I. Sezan and H. Stark. Tomographic image reconstruction from incomplete view data by convex projections and direct fourier inversion. *IEEE Trans. Medical Imaging*, MI-3(2): 91–98, 1984.

B. N. Shand, P. L. Starke, and G. de Jager. Limited angle tomography with lodox. Technical report, Digital Image Processing, University of Cape Town, 1998.

P. L. Starke and G. de Jager. Further work on limited angle tomography with lodox. Technical report, Digital Image Processing, University of Cape Town, 1998.

K. C. Tam and V. Perez-Mendez. Tomgraphical imaging with limited angle input. *J. Opt. Soc. Am.*, 71(5):582–192, 1981.

K. C. Tam, W. Eberhard, and K. W. Mitchell. Incomplete-data ct image reconstructions in industrial applications. *IEEE Trans. Nuclear Science*, 37(3):1490–1499, 1990.

R. J. Wilks. *Principles of Radiological Physics*. Churchill Livingstone, 1981.